Two Ways of Targeting a CD19 Positive Relapse of Acute Lymphoblastic Leukaemia after Anti-CD19 CAR-T Cells

Audrey Grain, Jocelyn Ollier, Thierry Guillaume, Patrice Chevallier, Baptiste Le Calvez, Marion Eveillard, Béatrice Clémenceau

biomedicines

MDPI

Brief Report

Two Ways of Targeting a CD19 Positive Relapse of Acute Lymphoblastic Leukaemia after Anti-CD19 CAR-T Cells

Audrey Grain [1,2,*], Jocelyn Ollier [1], Thierry Guillaume [3], Patrice Chevallier [3], Baptiste Le Calvez [3], Marion Eveillard [4] and Béatrice Clémenceau [1]

[1] Nantes Université, Inserm UMR 1307, CNRS UMR 6075, Université d'Angers, CRCI2NA, F-44007 Nantes, France
[2] Paediatric Haematology and Oncology Nantes University Hospital, 44093 Nantes, France
[3] Haematology Department, Nantes University Hospital, 44093 Nantes, France
[4] Haematology Biology Department, Nantes University Hospital, 44093 Nantes, France
* Correspondence: audrey.grain@chu-nantes.fr; Tel.: +33-2-40-08-36-14

Abstract: Background: Therapeutic options for CD19$^+$ relapses after anti-CD19 CAR-T cells are still debated; second infusion of anti-CD19 CAR-T cells, therapeutic antibodies, or targeted therapies can be discussed. Here, we explore the immunophenotyping and lysis sensitivity of CD19$^+$ ALL relapse after anti-CD19 CAR-T cells and propose different therapeutic options for such a high-risk disease. Methods: Cells from successive B-ALL relapses from one patient were collected. A broad immunophenotype analysis was performed. ^{51}Cr cytotoxic assays, and long-term killing assays were conducted using T-cell effectors that are capable of cytotoxicity through three recognition pathways: antibody-dependent cell-mediated cytotoxicity (ADCC), anti-CD19 CAR-T, and TCR. Results: Previously targeted antigen expression, even if maintained, decreased in relapses, and new targetable antigens appeared. Cytotoxic assays showed that ALL relapses remained sensitive to lysis mediated either by ADCC, CAR-T, or TCR, even if the lysis kinetics were different depending on the effector used. We also identified an immunosuppressive monocytic population in the last relapse sample that may have led to low persistence of CAR-T. Conclusion: CD19$^+$ relapses of ALL remain sensitive to cell lysis mediated by T-cell effectors. In case of ALL relapses after immunotherapy, a large immunophenotype will make new therapies possible for controlling such high risk ALL.

Keywords: acute lymphoblastic leukaemia; immunotherapy; relapse; CAR-T cells

Citation: Grain, A.; Ollier, J.; Guillaume, T.; Chevallier, P.; Le Calvez, B.; Eveillard, M.; Clémenceau, B. Two Ways of Targeting a CD19 Positive Relapse of Acute Lymphoblastic Leukaemia after Anti-CD19 CAR-T Cells. *Biomedicines* **2023**, *11*, 345. https://doi.org/10.3390/biomedicines11020345

Academic Editor: Myunggon Ko

Received: 6 January 2023
Revised: 20 January 2023
Accepted: 22 January 2023
Published: 25 January 2023

1. Introduction

T-cells expressing a chimeric antigen receptor (CAR) recognizing the CD19 antigen have shown high early response rates in high-risk B acute lymphoblastic leukaemia (B-ALL) [1]. Nevertheless, 35% to 44% of patients relapse, and more than 50% of them present CD19$^+$ relapses [2,3]. CD19$^+$ relapses are often related to low potency or low persistence of CAR-T cells [4]. Amplification and persistence of CAR-T cells may be negatively impacted by the choice of co-stimulatory domain, T-cell subtype composition, and an unfavourable immune environment [4,5]. Therapeutic options are still debated in the CD19$^+$ relapse setting: a second infusion of anti-CD19 CAR-T or antibodies targeting ALL have been proposed [6]. Humanised anti-CD19 CAR-T or associating a second infusion of anti-CD19 CAR-T cells with an anti-PD1 are other strategies explored in on-going Phase 1 studies [4,7–9].

To our knowledge, the susceptibility of ALL relapses to T-cells mediated lysis has not been explored so far. Here, we analyse broad immunophenotyping and cytotoxicity assays, conducted on ALL cells from successive relapses in one patient after three different immunotherapies in order to consider the optimal therapeutic way in this particularly complex setting.

2. Materials and Methods

2.1. Case Description

A 21-year-old patient presented with a hyperleukocytic CRLF2 overexpressing and IKZF1 deleted B-ALL (Dg) in November 2019. After failed induction chemotherapy combined with rituximab, intensification led to the first complete remission (CR) with positive minimal residual disease of 0.3% by multicolour flow cytometry (MFC) and 7×10^{-3} by molecular biology (based on Ig/TCR gene rearrangement). A geno-identical allogeneic HSCT was then performed. A relapse (R2) occurred 2 months later, and the patient received salvage chemotherapy followed by anti-CD19 CAR-T cells (tisagenlecleucel, 1.9×10^9 total viable cells, of which 9.4% were CAR^+ (based on the manufacturer's certificate) in July 2020. Bone marrow aspiration showed 81% of blasts before anti-CD19 CAR-T infusion. Circulating CAR-T cells in blood were detected using multicolour flow cytometry (MFC) and showed an expansion peak at day 8 (3.5% of T lymphocytes). Interestingly, the contemporary appearance of $CD14^+/HLA\text{-}DR^{lo/neg}$ monocytic cells was noted. A second CR was obtained with negative minimal residual disease at 1 month post-anti-CD19 CAR-T, persisting at 3 months post-infusion. The patient presented a loss of B cell aplasia at 4.5 months and a $CD19^+$ relapse at 5.5 months post-CAR-T cells (R3). He received palliative chemotherapy and died in January 2022 (Figure 1). The patient provided signed consent for cell collection.

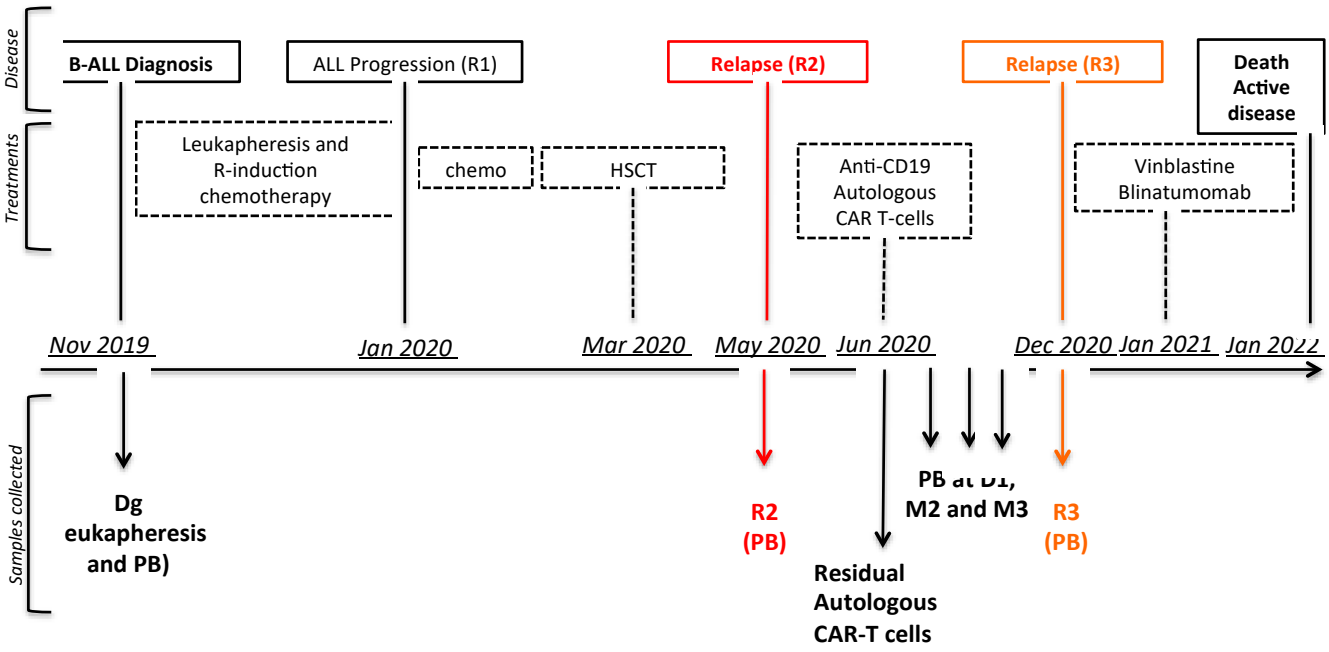

Figure 1. Clinical case medical history: disease progression, treatments received, and samples collected (Dg; R2; autologous CAR-T cells, blood samples and R3); ALL: acute lymphoblastic leukaemia; R: rituximab; HSCT: haematopoietic stem cell transplantation; PB: peripheral blood; chemo: chemotherapy.

2.2. Cells

At diagnosis, peripheral blood cells were collected from the leukapheresis product. Peripheral blood samples were collected at relapses R2 and R3. All contained at least 90% of blastic cells. Peripheral blood mononucleated cells (PBMC) were then isolated using density gradient centrifugation on a FICOLL-Paque solution (Eurobio). Cells were then frozen and used for experiments after thawing. The results could thus have been compared between relapses and initial diagnosis.

2.2.1. Cell Lines

Epstein-Barr B-lymphoblastoid cell lines (BLCL) were used as controls in all experiments and were derived from donor peripheral-blood mononuclear cells (PBMCs) following in vitro infection with EBV containing culture supernatant from the Marmoset B95-8 cell line in the presence of 1 µg/mL cyclosporin-A (sandimmun).

2.2.2. Effector Cells

- The patient's anti-CD19 CAR-T cells were collected from residual material in the bag after infusion of tisagenlecleucel. We performed an independent analysis of the cells in our laboratory. Of the $CD3^+$ cells, 11% were CAR^+. This result was close to that reported in the manufacturer certificate. The $CD4^+/CD8^+$ ratio among CAR^+ cells was 3.4 (77.5% $CD4^+$ and 22.3% $CD8^+$). CAR-T cells were largely composed of a differentiated T-cell subset, with $CD62L^+$, $CCR7^-$, and $CD45RA^-$ phenotypes.
- Because the tisagenlecleucel preparation only contained 9% of anti-CD19-CAR^+ T-cells, the anti-CD19-CAR^+ cells were selected with a CD19 biotin-coupled protein (Miltenyi Biotec). An APC-coupled anti-biotin antibody was then used for FACS-sorting the anti-CD19-CAR^+ cells. This T-cell population containing 95% of anti-CD19-CAR^+ T-cells (of which 71% were $CD8^+$ and 12% were $CD4^+$) was used for the cytotoxic assays. Note that the remaining 7% of $CD4^-$ and $CD8^-$ cells were composed of 72% of αβ-T lymphocytes and 28% of ϒδ-T lymphocytes.
- The anti-HLA-DPB1*04:01 $CD4^+$ T-clone has been previously described [10]. Cells were grown in RPMI 1640 culture medium (Eurobio) supplemented with 8% human serum, 300 IU/mL IL-2, 2 mM L-glutamine, penicillin, and streptomycin (Gibco).
- An anti-CMVpp65 polyclonal $CD8^+$-T-cell population was obtained as previously described [11] and grown in the same culture media.
- A $CD8^+$ polyclonal T cell population transduced by a retroviral vector expressing a chimeric-receptor containing the murine CD16 receptor murine FcɣRIII, linked to the human-chain FcεRIɣ, was obtained as previously described and used to perform antibody-dependent cell-mediated cytotoxicity (ADCC) assays with murine antibodies [12].

See all the effector cells in Supplementary Figure S1.

2.3. Immunophenotype

Extended immunophenotyping of Dg, R2, and R3 cells was performed using the Human Cell Surface Marker Screening Kit from Biolegend® ((Biolegend Europe B.V, Amsterdam, The Netherlands) (LEGENDscreen). The Human Cell Surface Marker Screening Kit contains 4 96-wells plates. Each well contains a PE-coupled antibody targeting one human surface antigen. Cells were first incubated with an anti-CD19-APC coupled antibody (Biolegend®, clone HIB19) in order to select the leukaemic blasts by gating $CD19^+$ cells for analysis. A minimum of 10 000 $CD19^+$ cells was acquired on a CANTO II cytometer (BD Biosciences, Le Pont de Claix, France) (Plateforme CytoCell–Nantes University), and the results were analysed using FlowJo v10.8.1 software (BD LifeSciences). Results were given in Relative Fluorescence Intensity (RFI in log) which is calculated as median fluorescence intensity of the targeted-antigen coupled antibody/median fluorescence intensity of the unspecific control isotype. All antigens screened in the panel are detailed in Supplementary Figure S2.

2.4. Cytotoxicity Assays

2.4.1. $^{51.}$ Cr Assays

In order to assess sensitivity to T-cells-induced lysis of each ALL sample, using different way of recognition (TCR, ADCC, CAR), standard 51Cr assay was first performed. Target cells were previously labeled with 75 µCi 51Cr for 1 h at 37 °C then washed 4 times with RPMI, SVF 10%. For cytotoxic assay using anti-CMV-pp65 $CD8^+$ T cells,

target cells were previously incubated for 30 min at 37 °C with 1µg/mL final concentration of CMVpp65 peptides pool (PepTivator CMV pp65 human) (Miltenyi Biotec SAS, Paris, France) and then washed twice. Target cells and effector T cells were then plated at the indicated effector-to-target ratio (E:T ratio) in flat-bottom 96 wells plates. A BLCL line was used as control. After a 4 h incubation at 37 °C, 25 µL of supernatant was removed from each well, mixed with 100 µL scintillation fluid (Ultima Gold XR) (PerkinElmer Health Sciences, Groninger, The Netherlands), and released 51Cr activity was counted in a scintillation counter (MicroBeta JET) (PerkinElmer Health Sciences, Groninger, The Netherlands). Each test was performed in triplicate. Results are expressed as the percentage of lysis, which is calculated according to the following equation: (experimental release − spontaneous release)/ (maximal release − spontaneous release) × 100. Three experiments in triplicate were performed independently.

2.4.1.1. Long-Term Killing Assays

Sensitivity to CAR-T induced lysis was analysed over 24 h because it better represents in vivo CAR-T activity [13]. Target (200,000 cells/well) and effector cells were plated at the E:T ratio 3:1 in a flat-bottom 96 wells plate and incubated at 37 °C. At different time points: 0 h (H0), 4 h (H4) and 24 h (H24) after co-culture, cell suspension was collected and wells were rinsed in order to collect all residual cells. Cells were then washed with PBS EDTA (0.02%) and with PBS before being labelled with a Fixable Viability Stain 780 (BD Biosciences) over 10 min at room temperature (RT). After having been washed twice, cells were then incubated with both a PE-coupled anti-CD22 antibody (Dako product provided by Technologies Agilent France, Les Ulis, France) and a FITC coupled anti-CD3 antibody (Beckman Coulter France SAS, Roissy, France) over 15 min RT, to distinguish effector and target residual viable cells. After two more washing with PBS-0.1% human albumin, cells were fixed before analysis by MFC. For each condition, the % of viable leukaemic cells ($VS780^{low}/CD22^{+}$) at time 0 was reported as 100%. Thus, at time 4 h and 24 h, the percentage of residual viable leukaemic cells was calculated as follows: = (% of viable CD22+ cells at this time/ % of viable CD22+ cells at H0) × 100.

Two experiments in duplicate were performed independently. All MFC analysis was performed on BD FACSCanto II (Plateforme CytoCell – Nantes University).

3. Results

3.1. ALL Immunophenotypes

Extended immunophenotyping showed that the level of expression of CD19 decreased from a Relative Fluorescence Intensity (RFI) of 171 at Dg, to 13 and 23 at R2 and R3, respectively. Expression of the previously targeted CD20 also decreased from Dg (RFI = 36) to R2 (RFI = 12) and R3 (RFI = 13). In contrast, CD22 was highly expressed in all samples.

Interestingly, while CD135 (FLT3) expression was present on only 7% of the Dg ALL cells, at relapse R2 its expression was observed on all the cells and was maintained at relapse R3. Similarly, CD268 (BAFF-R), CD304 (Neuropilin-1), and CD71 expressions increased on the successive relapse cells.

Expression of molecules involved in immunological synapse and co-stimulatory ligands remained stable, and expression of checkpoint inhibitors was low in all samples (Supplementary Figure S3).

The phenotypic analysis also revealed the presence of a monocytic $CD14^{+}$, $HLA\text{-}DR^{neg}$, $CD33^{+}$, and $CD11b^{high}$ population in the R3 relapse sample (3.8% of cells), and we showed that this population was detectable in the patient's peripheral blood 7 days after CAR-T cell infusion. The immunophenotype of these monocytic cells is presented in Supplementary Figure S4.

3.2. Lysis Sensitivity Mediated by T-Cells Using Different Recognition Pathways: Anti-CD19 -CAR, ADCC, and TCR:

3.2.1. The Anti-CD19 CAR Pathway

Four-hour ^{51}Cr cytotoxicity assays were performed, analysing the three ALL sample lyses induced by the FACS of CD19-CAR^{+} cells. All ALL samples were efficiently and similarly lysed by the patient's anti-CD19 CAR-T cells, even R3 (Figure 2a). The lysis scores were directly proportional to the effector–target ratio. The rapid lysis of all the ALL through the CAR recognition pathway was confirmed by the long-term killing assays. Only 0.5% of the residual viable CD22^{+} cells were seen after 4 h of co-culture (Figure 3b). The percentage of residual viable cells in the wells where ALL cells were cultured alone are presented as control (Figure 3a).

3.2.2. The ADCC Pathway

Four antigens, highly expressed by the three ALL (Dg, R2 and R3) were selected for the ADCC assays: CD19 (clone HIB19), CD24 (adhesion molecule, in B cells; clone ML5), CD184 (IL-4 receptor; clone 12G5), and CD220 (insulin receptor; clone B6.220). The mCD16-T lymphocytes were used as effector cells. For all targeted antigens, ADCC lysis scores ranged from 20% to 35% within four-hour ^{51}Cr cytotoxicity assays. In addition, ALL sensitivity to ADCC-mediated cell lysis remained stable from Dg to successive relapses, whatever antigen was targeted. No cell lysis was observed in the absence of antibodies (Figure 2d). Because of the lack of biological material, long-term killing assays could not be performed for ADCC.

3.2.3. The TCR Pathway

In the ^{51}Cr cytotoxicity assay, little or no ALL cell lysis was observed after co-culture with the anti-HLA DPB1*04:01 CD4^{+} T-clone or the anti-CMV^{pp65} CD8-polyclonal T-cells (Figure 2b,c). However, in the long-term killing assays, after 24 h of co-culture, the percentage of residual leukaemic viable CD22^{+} cells progressively fell to 30% in the presence of anti-CMV^{pp65} CD8-T cells and to 35% in the presence of the anti-HLA DPB1*04:01 CD4^{+} T-clone (Figure 3c,d). No significant difference in sensitivity to lysis was observed between ALL Dg and relapses. Note that in addition to the molecular HLA typing previously described, we checked with MFC that ALL cells maintained HLA-A2 and HLA-DPB1*04:01 expression (Figure 2b,c).

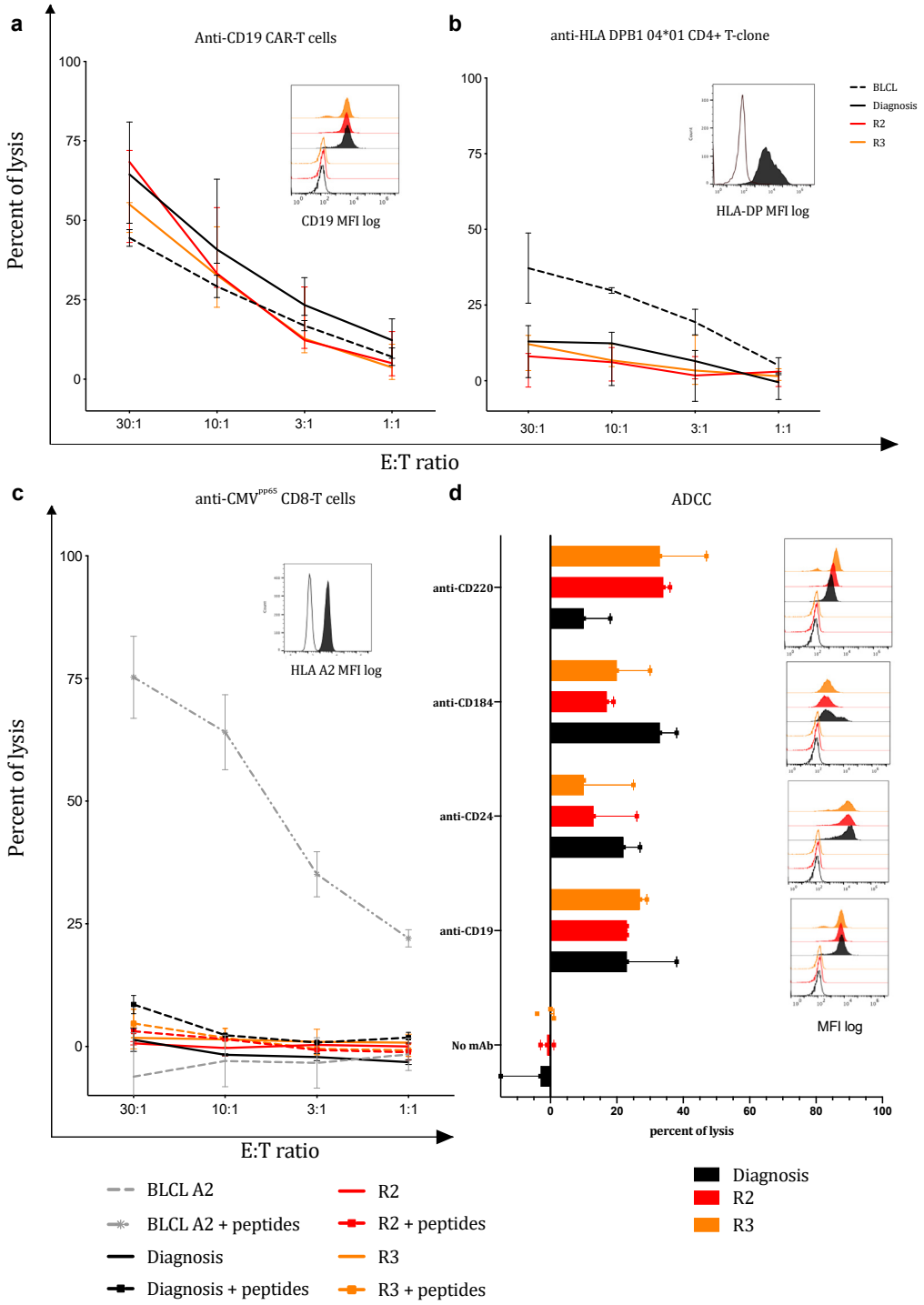

Figure 2. 4h-^{51}Cr cytotoxic assays over 4 h. Percentage of ALL lysis at four E:T ratio after co-culture with the autologous anti-CD19 CAR-T cell preparation (**a**); or anti-HLA DPB1*04:01 CD4+ T-clone (**b**); or anti-CMVpp65 CD8 T-cells (**c**); or through the ADCC pathway using anti-CD220, anti-CD184, anti-CD24, and anti-CD19 antibodies in combination with mCD16-T lymphocytes (**d**). Expressions of targeted antigens are, respectively, represented as median of immunofluorescence (MFI) in a log of 10. (BLCL: B cell lineage used as controls). Three experiments in triplicate were performed. Results are given as median/error.

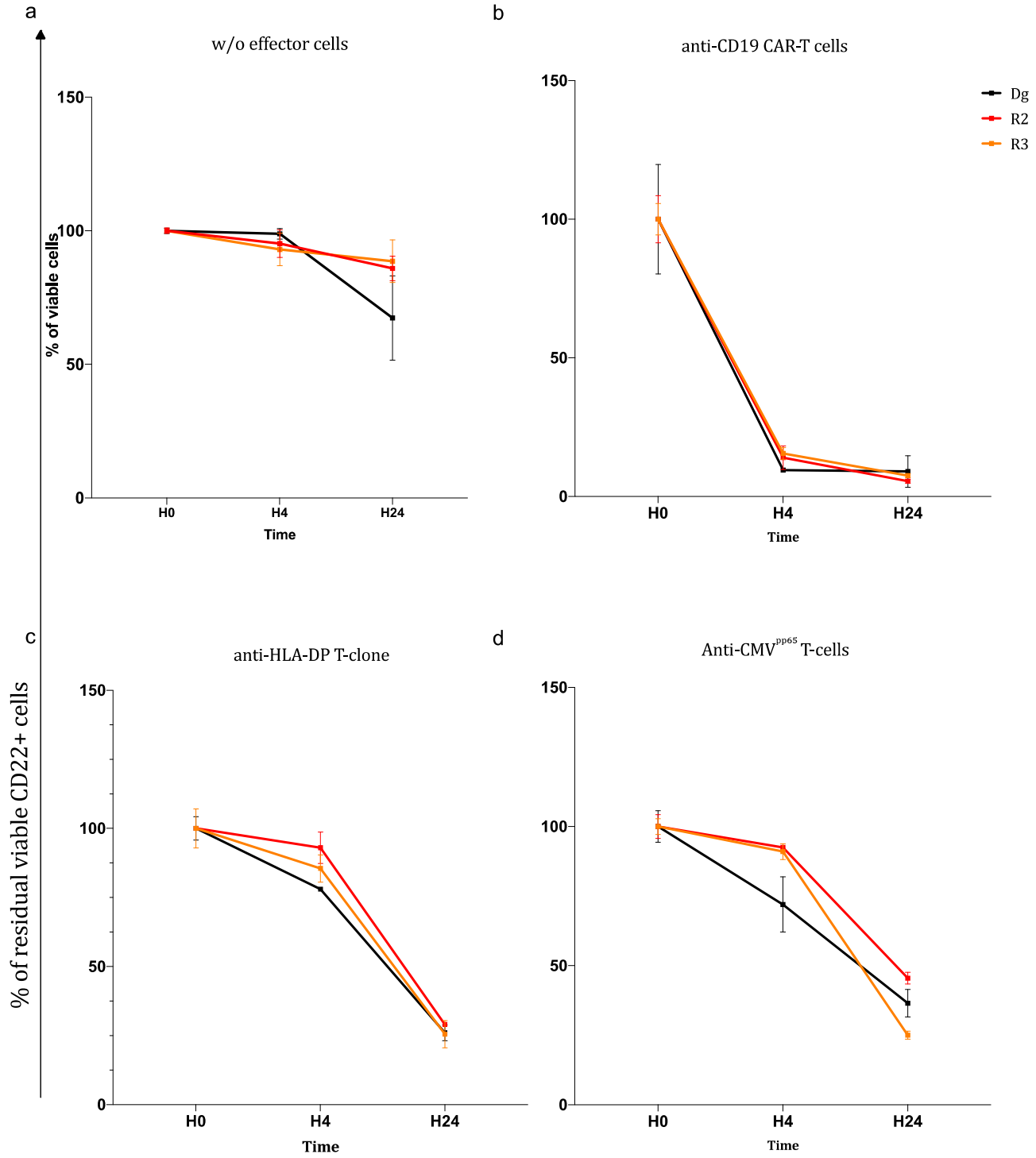

Figure 3. Long-term killing assays. Residual viable ALL cells at 3 time points of co-culture H0 (starting point), after 4 h (H4) of co-culture and after 24 h (H24) of co-culture: (**a**) with no effector, results showed total viable cells; (**b**) with a purified autologous anti-CD19 CAR-T cell preparation (percent of residual CD22+ viables cells); (**c**) with anti-HLA DPB1*04:01 CD4+ T-clone (percent of residual CD22+ viables cells); (**d**) with anti-CMVpp65 CD8 T-cells (percent of residual CD22+ viables cells). Two experiments in duplicate were performed at effector/ratio = 3:1. Results are given as mean + SD. CMVpp65 peptides: PepTivator CMVpp65 human, 130-093-435, Miltenyi Biotec; T eff: T-cell effectors, here polyclonal CD8+ T cells against CMV peptides.

4. Discussion

For the first time, we report here an analysis of the T-cell-mediated lysis sensitivity of two successive ALL relapses that occurred after three immunotherapies (rituximab, geno-identical allogeneic HSCT, and anti-CD19 CAR T-cells). We showed that ALL relapses remained sensitive to all cytotoxic T-cell effectors tested, which recognized ALL cells through different receptors (CAR, TCR, and CD16). Even if CD19 targeted antigen expression decreased in relapse samples, CAR-T cell-mediated lysis remained effective.

We did not identify the appearance of surface molecules that may impact CAR-T cell persistence. Meanwhile, some unexpected targetable antigens, not routinely tested, appeared between Dg and the successive relapses, including FLT3 (CD135) or BAFF-R (CD268). Overall, our results provide options for antibody- or cell-based immunotherapy in the setting of post-CAR-T CD19+ relapses.

The loss of CAR-T cells persistence is the first factor associated with $CD19^+$ ALL re-occurrence after anti-CD19 CAR-T cells. It is now well-known that the co-stimulatory domain impacts CAR-T persistence, as the CAR construct with 4-1BB is associated with longer persistence than the CD28 domain [4]. The patient described here received tisagenlecleucel (a 4-1BB anti-CD19 CAR construct). Because relapses remained sensitive to CAR-T cell-induced lysis, a second injection of tisagenlecleucel could therefore have been discussed. Nevertheless, published data from second anti-CD19 CAR-T cells infusions report disappointing results, mostly due to lack of expansion [6]. An unfavourable in vivo immune environment may also impact CAR-T expansion and persistence. The murine scFv of CAR could lead to immune rejection, and some groups are experimenting use of humanized or fully human CAR constructs [14,15]. In addition, lack of co-stimulatory molecules (CD80, CD86, ICAM-1) and expression of molecules leading to immune cell anergy (CD47, HLA-II or PD-L1) through leukaemic cells or the bone marrow microenvironment have also been described [16–20]. Therefore, pilot studies combining a second injection of CAR-T and a PD1 blockade were conducted, with encouraging results [7–9], and a Phase I/II study is ongoing (CAPTiRALL EUDRACTN: 2021-003035-28). Other strategies targeting pathways known to contribute to T-cell exhaustion were also explored with encouraging results (CTLA-4, TIM-3, TGF receptor) [21]. In our case, we did not find a lack of co-stimulatory molecules or expression of checkpoint inhibitors. Nevertheless, we identified the appearance of $CD14^+$/HLA-$DR^{lo/neg}$ monocytic cells in the R3 sample. Retrospectively, we noted that this monocytic population had appeared in peripheral blood since day 4 after tisagenlecleucel infusion. These monocytic $CD14^+$/HLA-$DR^{lo/neg}$ cells recently emerged as tumour-induced immunosuppression mediators and are associated with poorer CAR-T expansion during manufacturing [22–24]. Targeting this immunosuppressive monocyte population might therefore have improved responses to a potential second anti-CD19 CAR-T injection in this patient.

Our analysis of broad immunophenotyping revealed newly appeared targetable antigens in relapse samples and led to unexpected therapeutic options. For this patient, anti-FLT3 targeted therapy could thus have been discussed in a curative or pre-emptive setting. In addition, we also showed that ALL cells remain sensitive to ADCC-mediated lysis (antibody + mCD16-T lymphocytes). The mCD16-T lymphocytes are described as universal CAR-T cells because their construction allows targeting of multiple antigens when used in combination with different antibodies. These immunotherapeutic T-cells could be helpful for targeting both one or more leukaemic antigens and the immunosuppressive microenvironment.

In conclusion, our analysis of this refractory ALL revealed that, even in relapses, blastic cells remain sensitive to three-way T-cell-induced lysis. Moreover, we identified the appearance of new potential therapeutic targets in relapse samples. In light of our results, a second injection of anti-CD19 CAR-T could have been discussed. However, targeting the immunosuppressive microenvironment should probably have been considered. CD16-T-cells, seem particularly interesting in the post-conventional anti-CD19 CAR-T-cells relapse

setting, allowing the simultaneous targeting of several antigens, possibly identified by broad immunophenotyping.

Supplementary Materials: The following supporting information can be downloaded at: https://www.mdpi.com/article/10.3390/biomedicines11020345/s1, Figure S1: T-cell effectors used in the cytotoxicity assay. Figure S2: Antigens screened by the Human Cell Surface Marker Screening Kit from Biolegend®(LEGENDscreen). Figure S3: Immunophenotyping results. Figure S4: Cell surface antigen expressed by the monocytic population

Author Contributions: A.G., B.C., and J.O. conceived and performed the analysis. A.G. and B.C. wrote the manuscript. T.G. and B.L.C. treated the patient. P.C., M.E., B.L.C. critically reviewed the manuscript. All authors have read and agreed to the published version of the manuscript.

Funding: This research received no external funding.

Institutional Review Board Statement: Not applicable.

Informed Consent Statement: Written informed consent of the patient was preliminarily obtained for cell collection.

Data Availability Statement: Data are available on request from the corresponding author.

Acknowledgments: We thank the Cytometry Facility Cytocell in Nantes for expert technical assistance.

Conflicts of Interest: The authors declare no conflict of interest.

References

1. Maude, S.L.; Laetsch, T.W.; Buechner, J.; Rives, S.; Boyer, M.; Bittencourt, H.; Bader, P.; Verneris, M.R.; Stefanski, H.E.; Myers, G.D.; et al. Tisagenlecleucel in children and young adults with B-cell lymphoblastic leukemia. *N. Engl. J. Med.* **2018**, *378*, 439–448. [CrossRef] [PubMed]
2. Dourthe, M.E.; Rabian, F.; Yakouben, K.; Chevillon, F.; Cabannes-Hamy, A.; Méchinaud, F.; Grain, A.; Chaillou, D.; Rahal, I.; Caillat-Zucman, S.; et al. Determinants of CD19-positive vs CD19-negative relapse after tisagenlecleucel for B-cell acute lymphoblastic leukemia. *Leukemia* **2021**, *35*, 3383–3393. [CrossRef] [PubMed]
3. Grupp, S.A.; Maude, S.L.; Rives, S.; Baruchel, A.; Boyer, M.W.; Bittencourt, H.; Bader, P.; Büchner, J.; Laetsch, T.W.; Stefanski, H.; et al. Updated analysis of the efficacy and safety of tisagenlecleucel in pediatric and young adult patients with relapsed/refractory (r/r) acute lymphoblastic leukemia. *Blood* **2018**, *132*, 895. [CrossRef]
4. Nie, Y.; Lu, W.; Chen, D.; Tu, H.; Guo, Z.; Zhou, X.; Li, M.; Tu, S.; Li, Y. Mechanisms underlying CD19-positive ALL relapse after anti-CD19 CAR T cell therapy and associated strategies. *Biomark. Res.* **2020**, *8*, 1–17. [CrossRef] [PubMed]
5. Guha, P.; Cunetta, M.; Somasundar, P.; Espat, N.J.; Junghans, R.P.; Katz, S.C. Frontline Science: Functionally impaired geriatric CAR-T cells rescued by increased α5β1 integrin expression. *J. Leukoc. Biol.* **2017**, *102*, 201–208. [CrossRef] [PubMed]
6. Holland, E.M.; Molina, J.C.; Dede, K.; Moyer, D.; Zhou, T.; Yuan, C.M.; Wang, H.-W.; Stetler-Stevenson, M.; Mackall, C.; Fry, T.J.; et al. Efficacy of second CAR-T (CART2) infusion limited by poor CART expansion and antigen modulation. *J. Immunother. Cancer* **2022**, *10*, e004483. [CrossRef] [PubMed]
7. Maude, S.L.; Hucks, G.E.; Seif, A.E.; Talekar, M.K.; Teachey, D.T.; Baniewicz, D.; Callahan, C.; Gonzalez, V.; Nazimuddin, F.; Gupta, M.; et al. The effect of pembrolizumab in combination with CD19-targeted chimeric antigen receptor (CAR) T cells in relapsed acute lymphoblastic leukemia (ALL). *J. Clin. Oncol.* **2017**, *35*, 103. [CrossRef]
8. JJaeger, U.; Worel, N.; McGuirk, J.; Riedell, P.A.; Fleury, I.; Borchmann, P.; Du, Y.; Abdelhady, A.M.; Han, X.; Martinez-Prieto, M.; et al. Safety and efficacy of tisagenlecleucel (tisa-cel) plus pembrolizumab (pembro) in patients (pts) with relapsed/refractory diffuse large B-cell lymphoma (r/r DLBCL): Updated analysis of the phase 1b PORTIA study. *J. Clin. Oncol.* **2021**, *39*, e19537. [CrossRef]
9. Cao, Y.; Lu, W.; Sun, R.; Jin, X.; Cheng, L.; He, X.; Wang, L.; Yuan, T.; Lyu, C.; Zhao, M. Anti-CD19 chimeric antigen receptor T cells in combination with nivolumab are safe and effective against relapsed/refractory B-cell non-Hodgkin lymphoma. *Front. Oncol.* **2019**, *9*, 767. [CrossRef]
10. Vivien, R.; Saïagh, S.; Lemarre, P.; Chabaud, V.; Jesson, B.; Godon, C.; Jarry, U.; Guillaume, T.; Chevallier, P.; Vié, H.; et al. The doubling potential of T lymphocytes allows clinical-grade production of a bank of genetically modified monoclonal T-cell populations. *Cytotherapy* **2018**, *20*, 436–452. [CrossRef]
11. Gallot, G.; Vivien, R.; Ibisch, C.; Lulé, J.; Davrinche, C.; Gaschet, J.; Vié, H. Purification of Ag-specific T lymphocytes after direct peripheral blood mononuclear cell stimulation followed by CD25 selection. I. Application to CD4+ or CD8+ cytomegalovirus phosphoprotein pp65 epitope determination. *J. Immunol.* **2001**, *167*, 4196–4206. [CrossRef] [PubMed]
12. Ollier, J.; Vivien, R.; Vié, H.; Clémenceau, B. Transfection of FcγRIIIa (CD16) Alone Can Be Sufficient To Enable Human αβTCR T Lymphocytes To Mediate Antibody-Dependent Cellular Cytotoxicity. *ImmunoHorizons* **2017**, *1*, 63–70. [CrossRef]

13. Liu, D.; Badeti, S.; Dotti, G.; Jiang, J.G.; Wang, H.; Dermody, J.; Soteropoulos, P.; Streck, D.; Birge, R.B.; Liu, C. The role of immunological synapse in predicting the efficacy of chimeric antigen receptor (CAR) immunotherapy. *Cell Commun. Signal.* **2020**, *18*, 134. [CrossRef]
14. Cao, J.; Cheng, H.; Shi, M.; Wang, G.; Chen, W.; Qi, K.; Li, H.; Qiao, J.; Zhao, J.; Wu, Q.; et al. Humanized CD19-specific chimeric antigen-receptor T-cells in 2 adults with newly diagnosed B-cell acute lymphoblastic leukemia. *Leukemia* **2019**, *33*, 2751–2753. [CrossRef] [PubMed]
15. Maude, S.L.; Barrett, D.M.; Rheingold, S.R.; Aplenc, R.; Teachey, D.T.; Callahan, C.; Shaw, P.A.; Brogdon, J.; Young, R.; Scholler, J.; et al. Efficacy of humanized CD19-targeted chimeric antigen receptor (CAR)-modified T cells in children with relapsed ALL. *J. Clin. Oncol.* **2016**, *34*, 3007. [CrossRef]
16. Jiménez-Morales, S.; Aranda-Uribe, I.S.; Pérez-Amado, C.J.; Ramírez-Bello, J.; Hidalgo-Miranda, A. Mechanisms of Immunosuppressive Tumor Evasion: Focus on Acute Lymphoblastic Leukemia. *Front. Immunol.* **2021**, *12*, 737340. [CrossRef] [PubMed]
17. Kang, S.H.; Hwang, H.J.; Yoo, J.W.; Kim, H.; Choi, E.S.; Hwang, S.H.; Cho, Y.U.; Jang, S.; Park, C.J.; Im, H.J.; et al. Expression of immune checkpoint receptors on T-cells and their ligands on leukemia blasts in childhood acute leukemia. *Anticancer Res.* **2019**, *39*, 5531–5539. [CrossRef]
18. Kebelmann-Betzing, C.; Körner, G.; Badiali, L.; Buchwald, D.; Möricke, A.; Korte, A.; Köchling, J.; Wu, S.; Kappelmeier, D.; Oettel, K.; et al. Characterization of cytokine, growth factor receptor, costimulatory and adhesion molecule expression patterns of bone marrow blasts in relapsed childhood B cell precursor all. *Cytokine* **2001**, *13*, 39–50. [CrossRef]
19. Luczyński, W.; Stasiak-Barmuta, A.; Iłendo, E.; Kovalchuk, O.; Krawczuk-Rybak, M.; Malinowska, I.; Mitura-Lesiuk, M.; Chyczewski, L.; Matysiak, M.; Kowalczyk, J.; et al. Low expression of costimulatory molecules and mRNA for cytokines are important mechanisms of immunosuppression in acute lymphoblastic leukemia in children? *Neoplasma* **2006**, *53*, 301–304.
20. Simone, R.; Tenca, C.; Fais, F.; Luciani, M.; De Rossi, G.; Pesce, G.; Bagnasco, M.; Saverino, D. A soluble form of CTLA-4 is present in paediatric patients with acute lymphoblastic leukaemia and correlates with CD1d+ expression. *PloS ONE* **2012**, *7*, e44654. [CrossRef]
21. Titov, A.; Kaminskiy, Y.; Ganeeva, I.; Zmievskaya, E.; Valiullina, A.; Rakhmatullina, A.; Petukhov, A.; Miftakhova, R.; Rizvanov, A.A.; Bulatov, E. Knowns and Unknowns about CAR-T Cell Dysfunction. *Cancers* **2022**, *14*, 1078. [CrossRef] [PubMed]
22. Bourbon, E.; Sesques, P.; Gossez, M.; Tordo, J.; Ferrant, E.; Safar, V.; Wallet, F.; Aussedat, G.; Maarek, A.; Bouafia, F.; et al. HLA-DR expression on monocytes and outcome of anti-CD19 CAR-T cell therapy for large B-cell lymphoma. *Blood Adv.* 2022. [CrossRef] [PubMed]
23. Mengos, A.E.; Gastineau, D.A.; Gustafson, M.P. The CD14+HLA-DRlo/neg Monocyte: An Immunosuppressive Phenotype That Restrains Responses to Cancer Immunotherapy. *Front. Immunol.* **2019**, *10*, 1147. [CrossRef] [PubMed]
24. Stroncek, D.F.; Ren, J.; Lee, D.W.; Tran, M.; Frodigh, S.E.; Sabatino, M.; Khuu, H.; Merchant, M.S.; Mackall, C.L. Myeloid cells in peripheral blood mononuclear cell concentrates inhibit the expansion of chimeric antigen receptor T cells. *Cytotherapy* **2016**, *18*, 893–901. [CrossRef] [PubMed]

SUPPLEMENTARY MATERIAL:

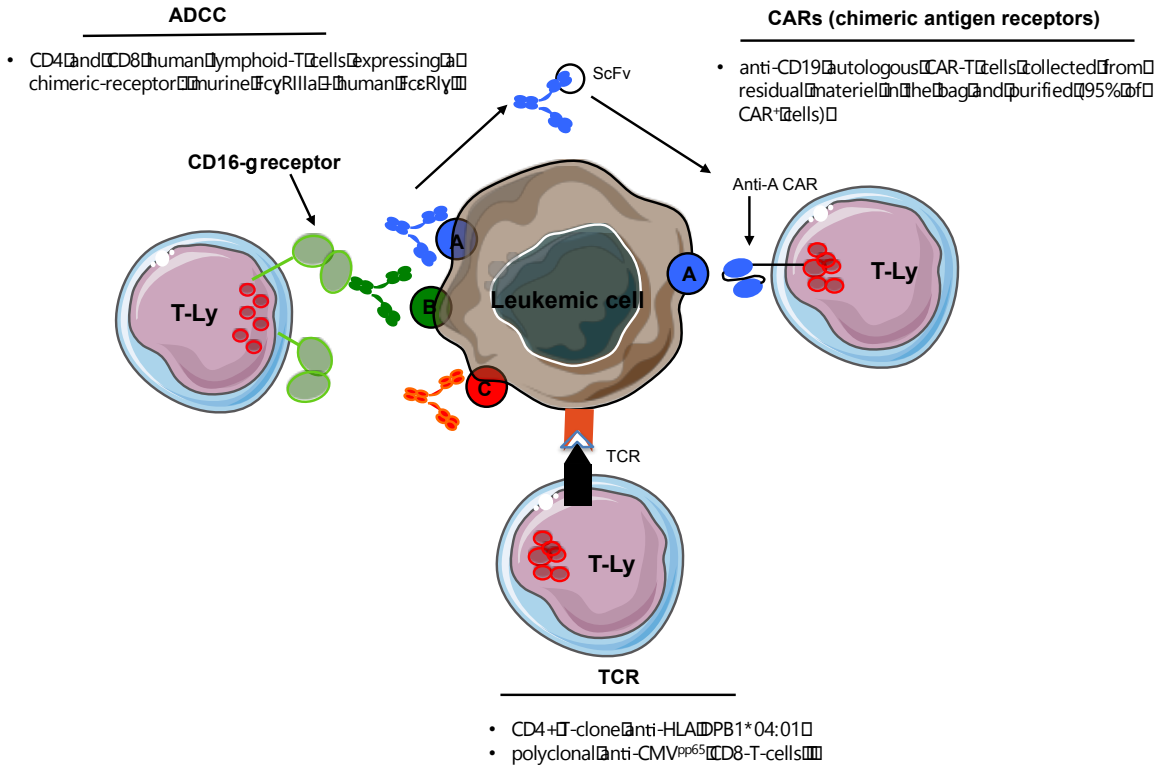

Figure S1: T-cell effectors used in the cytotoxicity assay. To compare the lysis sensitivity of each ALL, some T-lymphoid effectors were used, capable of inducing targeted cell death via different mechanisms: purified autologous anti-CD19 CAR-T cells inducing lysis through CD19 recognition by the CAR; CD4+ T-clone anti-HLA DPB1*04:01 and polyclonal anti-CMVpp65 CD8-T-cells inducing cell lysis through the TCR; and CD4 and CD8 human lymphoid T-cells transduced by a lentiviral vector, expressing a chimeric-receptor containing the murine CD16 receptor inducing cell lysis when combined with murine antibodies through the ADCC mechanism.

BLANK	CD244	DLL1	HLA-DR
Hamster IgG ctrl	CD245	DLL4	Ig light chain lambda
CCR10	CD25	DR3	IgD
CD278	CD252	EGFR	IL-28RA
IFN-gRb	CD261	GITR	Integrin b5
Mouse IgG1 ctrl	CD262	GPR19	KLRG1
CD46	CD263	GPR56	LOX-1s
CD70	CD266	HLA-Es	MICA-MICB
CD1a	CD268	HVEM	MSC W3D5
CD2	CD27	Ig light chain kappa	Notch-2
b2m	CD271	IgM	TACSTD2
B7-H4	CD275	IL-21R	TIGIT
Cadherin 11	CD276	Integrin a9b1	Mouse IgG2b ctrl
CD10	CD277	Jagged 2	C3AR
CD100	CD279	Ksp37	CCX-CKR
CD103	CD28	LAP	CD11c
CD105	CD29	LY6G6D	CD129
CD106	CD290	MERTK	CD158
CD107a	CD298	MSC W7C6	CD181
CD107b	CD3	MSC NPC W4A5	CD193
CD109	CD30	MSCA	CD196
CD111	CD300c	MUC-13	CD1d
CD112	CD309	NKp80	CD20
CD114	CD31	Notch-1	CD22
CD116	CD314	Notch-3	CD220
CD117	CD317	Notch-4	CD235ab
CD119	CD324	NPC	CD258
CD11a	CD325	NTB-A	CD274
CD11b	CD328	PSMA	CD319
CD122	CD33	ROR1	CD32
CD123	CD334	Siglec-10	CD326
CD126	CD335	Siglec-7	CD338
CD127	CD336	Siglec-8	CD368
CD13	CD337	Siglec-9	CD45RA
CD131	CD34	SSEA-5	CD45RB
CD134	CD340	SUSD2	CD49e
CD135	CD344	TCRab	CD52
CD137	CD35	TCR gd	CD66ace
CD137L	CD354	Tim-4	CD85h
CD138	CD360	TLT-2	CD85j
CD14	CD365	TM4SF20	CD86
CD140a	CD366	TRA-2-49	CD92
CD140b	CD367	TRA-2-54	CXCR7
CD141	CD36L1	TSLPR	Delta opioid R
CD142	CD38	VEGFR3	DRD1
CD143	CD39	Mouse IgG2a ctrl	EphA2
CD146	CD4	APCDD1	FceRIa
CD148	CD40	BTLA	GARP
CD15	CD41	CCR8	IL-15Ra
CD150	CD42b	CCRL2	LT-bR
CD151	CD43	CD102	MRGX2
CD154	CD44	CD104	TMEM8A
CD156c	CD45	CD124	CD254
CD158e1	CD47	CD130	CD318
CD16	CD48	CD144	Mouse IgG3 ctrl
CD161	CD49a	CD152	CD255
CD162	CD49b	CD155	SSEA-4
CD163	CD49c	CD158b	Mouse IgM ctrl
CD164	CD49d	CD184	Sialyl Lewis X
CD165	CD5	CD186	TRA-1-80
CD166	CD50	CD192	CD160
CD169	CD54	CD197	CD57
CD170	CD55	CD199	CD66b
CD172ab	CD56	CD209	TRA-1-60R
CD172g	CD58	CD217	Rat IgG1 ctrl
CD178	CD6	CD230	CD115
CD179a	CD61	CD24	CD201
CD179b	CD62E	CD243	Rat IgG2a
CD18	CD62L	CD26	CD120b
CD180	CD62P	CD269	CD210
CD182	CD63	CD282	CD267s
CD183	CD64	CD284	CD294
CD185	CD69	CD301	CD49f
CD19	CD73	CD303	CD85a
CD191	CD74	CD304	CD85d
CD194	CD79b	CD307	IgG Fc
CD1b	CD8	CD323	Integrin b7
CD1c	CD80	CD357	XCR1
CD200	CD81	CD36	Podoplanin
CD200R	CD82	CD369	Rat IgG2b ctrls
CD202b	CD83	CD370	CD132
CD203c	CD85g	CD371	CD195
CD205	CD85k	CD45RO	CX3CR1
CD206	CD87	CD51	Rat IgM ctrl
CD207	CD89	CD59	SSEA-3
CD21	CD8a	CD7	
CD213a1	CD9	CD71	
CD213a2	CD90	CD84	
CD218a	CD93	CD88	
CD221	CD94	CRTAM	
CD223	CD95	HER-3	
CD226	CD96	FPR3	
CD227	CD97	Ganglioside GD2	
CD229	CD99	GPR83	
CD23	CXCL16	HLA-ABC	
CD231			

Figure S2: Antigens screened by the Human Cell Surface Marker Screening Kit from Biolegend® (LEGENDscreen). Each plaque was detailed in one column.

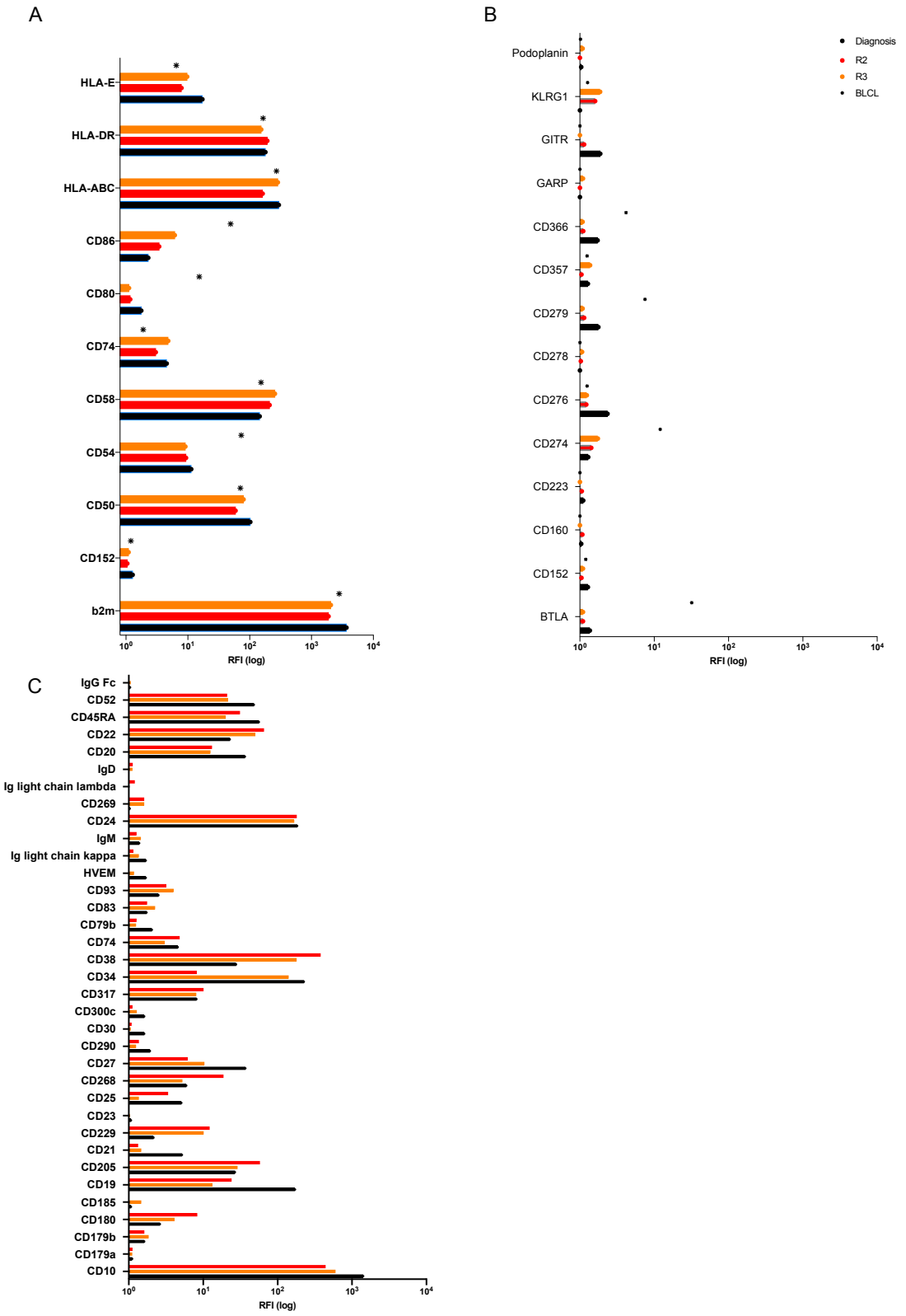

Figure S3: Immunophenotyping results: Immunophenotyping results for the 3 ALL: at diagnosis (Dg), post-HSCT relapse (R2) and post-CAR-T relapse (R3). A: molecules involved in the immunological synapse; B: checkpoint inhibitors and C: B-cells markers. The immunophenotype of a B-EBV induced cell line (BLCL) was presented as a control.

CD205; CD200R; CD183; CD18; CD179a; CD172αβ; CD170; CD16; CD156c; CD15; CD14; CD137L; CD13; CD11b; CD11a; CD107a; β2microglobulin; CCR10; CD97; CD95; CD93; CD89; CD82; CD74; CD64; CD63; CD58; CD55; CD50; CD48; CD47; CD45; CD44; CD43; CD367; CD354; CD35; CD33; CD31; CD298; CD277; CD27; CD263; Class I HLA; GPR83; GD2; FPR3; CD88; CD59; CD45RO; CD371; CD369; CD301; CD284; CD282; CD269; CD243; CD24; CD217; CD199; CD197; CD184; CD158b; CCR8; TM4SF20; TCRαβ; Siglec-8; MSC (W7C6); IL-21 R; CD195; CD132; CD85d; CD85a; CD49f; CD294; CD210; CD120b; CD201; CD115; CD66b; Sialyl Lewis X; CD92; CD66ace; CD368; CD32; CD274; CD181; CD11c; MSC (W3D5); LOX-1s; Integrinβ5.

Figure S4: Cell surface antigen expressed by the monocytic population isolated from the R3 sample.